PROF. J. VLCEK*
University of Toronto
Toronto 5, Canada

Systematic Errors of Image Coordinates

The proposed method will introduce randomness into the orientation parameter errors that arise from atmospheric refraction, lens and film distortions, and comparator errors.

(*Abstract on next page*)

INTRODUCTION

THE CORRECTION OF image coordinates of points on aerial photographs is a procedure whereby the location of a point on the photograph is slightly altered by numerical methods in the hope that its new position will be a better approximation of its *true* position which is usually defined by an ideal central projection. Systematic errors or biases of the coordinates are caused by many factors which play varied roles during the execution of the photographic and measuring phase prior to the analytical slution. The effects of some of these factors which affect image locations are known with a reasonably high degree of accuracy, and can be predicted and treated analytically. Other factors produce effects which, although detectable, are extremely difficult to deal with numerically. An example here may be lack of flatness of film during exposure. Although experimental studies (Clark 1964) reveal considerable distortions resulting from this cause, numerical compensation seems practically impossible in the majority of contemporary cameras which are equipped only with fiducial marks. The hope here appears to be the elimination of this defect at its source or employment of the reseau technique.

The major sources of image dislocations that are amenable to numerical compensation with varying degrees of success are: atmospheric refraction, lens distortion, film distortion and comparator errors. Although a number of articles has appeared in the literature on these individual topics, very little has been reported on the overall degree of improvement in the analytical solution as a result of application of corrections. This is despite the widely accepted opinion among photogrammetrists that the very advantage of the analytical over the instrumental solution is the possibility of correcting the various biases of image point coordinates. Evidently, success seems to follow very slowly. The progress is hampered, in part, by lack of adequate and reliable data most of which have to be acquired through lengthy and tedious experimental procedures. Corrective methods proposed on the basis of insufficient data quite often worsen rather than improve the situation.

It is obvious that any significant improvement in the accuracy of the photogrammetric solution has to come through the gradual elimination or lessening of the various sources of inaccuracies of the coordinates. This is one of the major problems facing aerial photogrammetry today. In the meantime it is de-

PROF. J. VLCEK

* Submitted under the title "Systematic errors of image coordinates, their compensation and consequences."

sirable to utilize all the means that keep the damage from this cause at a minimum.

In the following, some of the sources of coordinate biases will be discussed and experimental results obtained at the University of Toronto will be given. At the end, a statistical model will be given for the picture coordinate errors and a proposal will be made for selection of points for analytical solution.

Atmospheric Refraction

It is customary, for the purpose of calculating photogrammetric refraction, to assume certain simplifications regarding the geometric and physical models for the earth, the atmosphere and the photograph. Some of the assumptions are necessary because of lack of supporting data, others are justified in view of practical applications of aerial photography. For instance, it can and has been shown analytically that the effect of earth curvature upon refraction can be neglected for flying heights commonly employed in practical photogrammetry.

A more complicated problem concerns the physical model for the atmosphere existing at the time and place of photography. In the absence of local meteorological data the existence of a standard or model atmosphere is normally assumed on which the refraction calculation is based. Because the tilt of the photograph and topography of the terrain are unknown at the time of application of the corrections, vertical pictures and flat terrain are also assumed. Finally, the dynamic state of the atmosphere will probably forever remain unknown to the photogrammetrist. Fortunately, photography is usually not taken under turbulent air conditions.

Under these assumptions, the calculated displacement caused by refraction can only be an approximation. The question is, of course, how good the approximation is. Apart from the unknown composition of the atmosphere and its dynamic state at the moment of exposure the various assumptions mentioned above introduce errors whose magnitude, or at least their bounds, can be determined.

Our study of photogrammetric refraction concerned itself with the departure of actual atmosphere from the model atmosphere and its effect upon the calculation of the displacement. For this purpose we analysed various samples of radiosonde measurements of temperature, pressure and relative humidity obtained from meteorological balloons (Turner 1968). These data, measured at specific heights above terrain, were used to calculate, according to a formulation given by Owens (1967), the indices of refraction for each point. The refractive index-altitude profiles were then passed through these points using curve fitting procedures and numerical integration was employed to evaluate the integral:

$$R = k \int_{H_0}^{H} (n^2 - k^2)^{-1/2} dH \qquad (1)$$

where

R = distance on the ground from the point in question to the ground principal point,
H = height of camera,
H_0 = height of terrain,
n = index of refraction as a function of altitude,
$k = n \sin \theta$, θ = angle between the ray and the vertical at the camera station.

Formula 1 is valid for flat terrain, horizontal air strata and vertical photographs. The displacement d of the point on the photograph can then be calculated from:

$$d = r - \frac{Rf}{H - H_0} \qquad (2)$$

where

r = radial distance of point on the picture from its principal point,
f = camera constant.

The study revealed no appreciable differences

Abstract: *The author studies the systematic errors of image point coordinates that can be numerically compensated, namely those caused by atmospheric refraction, lens distortion, film distortion and comparator errors, and presents results of research in this area obtained at the University of Toronto. At the end, he develops a statistical model for the coordinates and proposes a way of selection of points for the analytical solution so that the adverse effect of the remaining systematic errors will be minimized.*

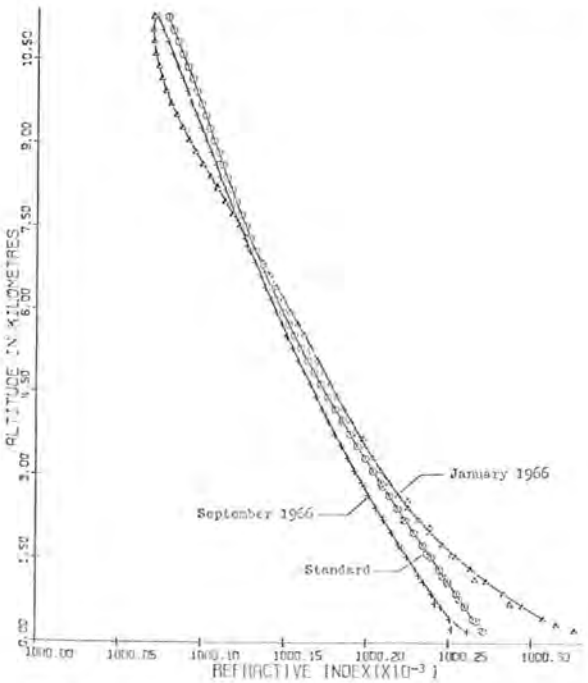

FIG. 1. Profile of the index of refraction for the U. S. Standard Atmosphere and two extreme sample atmospheres based on the 1966 records of Trout Lake weather station in Canada.

in the photogrammetric refraction calculated from the actual atmospheric data or using values given for the standard atmosphere for flying heights up to about 15,000 feet. Only for greater flying heights and for large zenith angles the departures from standard atmosphere begin to show appreciable discrepancies. As an illustration, Figure 1 shows the index of refraction profile for the U. S. Standard Atmosphere and two extreme sample atmospheres based on the 1966 records of the Trout Lake weather station in Canada. As the index of refraction is influenced mainly by temperature, these two profiles represent the warmest and coldest clear days of the year. In Figure 2 are shown the corresponding curves of refraction displacements as functions of radial distance for a vertical picture, $H=$ 35,000 feet and $f=152$ mm. It can be seen that the maximum discrepancy between the standard and the sample atmosphere displacements is about 3 microns for a ray inclined 45° from vertical.

Although on a truly vertical photograph the refraction displacement is expressible simply as a function of the radial distance from the principal point, the problem is more difficult on a tilted photograph and is further complicated by changes of relief. Because tilt and topographical data are not available prior to the analytical solution, the calculation of refraction corrections based on the radial distance from the principal point is only approximate. However, error bounds can be determined assuming certain extreme situations: e. g. for a 3° tilt, $H=35{,}000$ feet and 0.05 H elevation change and $f=150$ mm., the error can be as much as 10 microns.

The most difficult refraction to evaluate is that caused by air turbulance, especially near the camera. Air turbulance causes the path of the light ray to become a space curve rather than a plane curve. Practically nothing is known about the magnitude of errors arising from this source, because it is difficult to obtain such data under the actual conditions of photography although it has been shown experimentally (Vlcek 1968) that such errors are not significant within small areas of the film which might be expected.

In conclusion, although the present way of correcting photogrammetric refraction on the basis of simplified models appears adequate, especially for medium- and low-altitude photography, it is only a comparison with other systematic errors of the coordinates which are much larger at the present time. On the other hand, lessening or elimination of the major

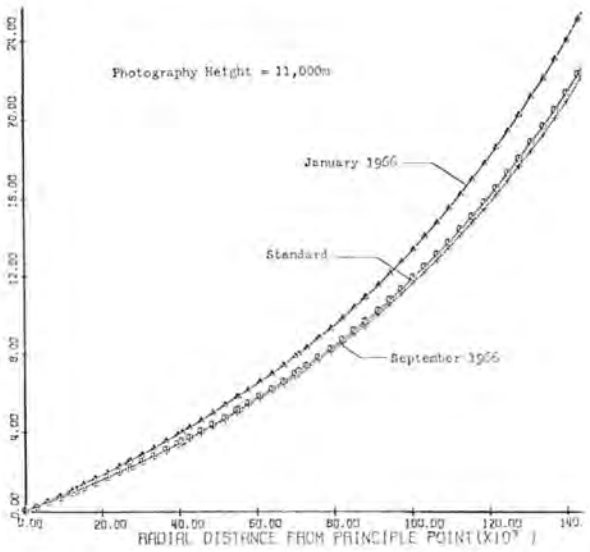

FIG. 2. Image displacement for the refraction curves of Figure 1 at $H=35{,}000$ feet and $f=152$ mm.

sources of errors, particularly dimensional instability or emulsion carriers and lack of their flatness will make the refraction errors more prominent; in fact, they may become the ultimate limiting factor in photogrammetric accuracy in years to come.

LENS DISTORTION

The results of camera calibration usually consist of values of distortion at discrete points along the diagonals of the picture format. The problem of the photogrammetrist is to devise, on the basis of these data and the theoretical considerations concerning the nature of the distortion, a suitable method of interpolating these values within the region of the image plane.

If the point of autocollimation is used as the origin of picture coordinates, which is commonly done, the distortion can be viewed as a vector displacement whose magnitude and direction varies both radially and azimuthally within the picture field. Although it is not absolutely necessary, it is customary to treat the radial and tangential components of the displacement vector separately. Only the former has been commonly subjected to correction so far but with the improvement of the calibration methods and with the insistence of the analytical photogrammetrist on a more thorough distortion calibration the tangential component ought to be corrected also.

The model which we are using at the present time in Toronto for correction of the radial distortion d_r is of the form:

$$\begin{aligned} d_r &= b_1 r + b_2 r^3 + b_3 r^5 + \cdots \\ &\quad + c_1 r^2 \cos(\theta_0 + \theta) + \cdots \\ &\cong b_1 r + b_2 r^3 + b_3 r^5 \\ &\quad + a_1 r^2 \cos\theta + a_2 r^2 \sin\theta \end{aligned} \tag{3}$$

where

r = radial distance
θ = azimuth angle
θ_o = unknown constant angle.

The terms with the b-coefficients describe the nature of the calibrated radial symmetric distortion which is one of the uncompensated Seidel aberrations. The terms with the a-coefficients describe, to a first-degree approximation, the nature of the asymmetric radial distortion which is caused by imperfect centering of the individual lenses on one optical axis. The theory of aberrations caused by lens decentering was dealt with in optical literature by Maréchal (1950), Stephan (1949), Epstein (1950), Conrady (1919) and others.

All the coefficients of Equation 3 are estimated in one least-square solution involving all data. As an example, calibration data pertaining to two wide-angle Wild cameras equipped with Aviogon lenses yielded estimates of the standard errors of radial distortion of ± 2.1 and ± 1.9 microns obtained from the residuals after fitting Model 3. Figure 3 illustrates the results for the second lens. In a recent paper, Karren (1968) gives the value of ± 2 microns as the standard error in radial distortion obtained from the evaluation study

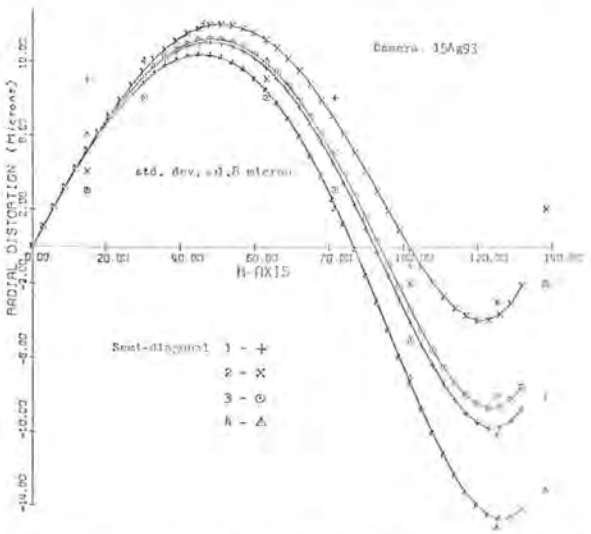

FIG. 3. Symmetric radial distortion along the four semi-diagonals of a lens field.

of the multi-collimator method of aerial camera calibration at the U. S. Geological Survey.

It might be of interest to note that considerable simplicity exists in the solution by Equation 3 as a result of the symmetry of the calibration data and the orthogonality of the sine and cosine functions. As a consequence, the radial symmetric and the radial asymmetric distortion components are statistically independent; moreover, the submatrix of the normal equation and its inverse which relates to the a-coefficients is a constant diagonal matrix (i.e., its two diagonal elements are the same). This assures that the variance of the radial distortion d_r given by Equation 4 is a radially symmetric function about the point of autocollimation:

$$\text{var}\,(d_r) = u^T N^{-1} u \sigma^2 \qquad (4)$$

where

$u^T = (r \quad r^3 \; r^5 \; r^2 \cos\theta \quad r^2 \sin\theta)$
N^{-1} = inverse of the normal matrix
σ^2 = variance of the observations estimated from the residuals.

It should be mentioned that the variance of the observations reflects the errors in measured radial distances, the errors in measured collimator angles and the random deviations caused by the lens system itself, such as glass imperfections, geometrically imperfect lens surfaces etc. The variance of the observations is likely to vary along the semidiagonal, increasing from the centre. This heterogeneity ought to be taken into account in the solution by a suitable covariance matrix of the observations.

The tangential distortion can be treated similarly to the asymmetric radial distortion by establishing a suitable functional relationship for the tangential profile which varies in azimuth as the sine of the angle. To the first approximation the model for tangential distortion d_t is

$$d_t = c_1 r^2 \sin\theta + c_2 r^2 \cos\theta. \qquad (5)$$

Sufficient data have not been published to give a practical value for the precision of tangential distortion but it is likely that it will be lower than that of the radial distortion.

FILM DISTORTION

Film distortion is one of the most serious limiting factors of the accuracy of the photogrammetric solution and one of the most difficult to eliminate analytically in cameras with only fiducial marks. The primary causes of this distortion are the dimensional changes of the film base which undergoes various temporary and permanent changes from the instant of the formation of the latent image during the exposure until the time that the developed image is finally transferred onto the glass diapositive.

Film distortion has been studied by many investigators, although nowhere could be found an analysis in which the true nature of the distortion was completely determined by a statistical separation of the systematic and random components of the displacement vec-

tor. Usually, various mathematical models were selected on the basis of *a priori* considerations and experimental data fitted to these models with the aim of showing their effectiveness in removing the distortion.

Our study was designed to reveal an exact analytical form of the film distortion caused by processing and therefore show its variation along the film roll. The study was conducted on Dupont polyester *Cronar* base film and consisted of copying a grid plate on the film and transferring the developed images onto diapositives which were then measured along with the original grid on our Wild stereocomparator in such a way that the discrepancies between the master grid and the copies were free, insofar as possible, of major comparator errors. A method of analysis using orthogonal polynomials (Vlcek 1965) was employed to separate the systematic and the random components of the discrepancies. This method is particularly suitable for this analysis, because it is extremely simple to apply and has very useful statistical properties. The assumption is, of course, that the film distortion can be represented by polynomials. This assumption does not appear unreasonable. The x- and y-components of the discrepancies were treated separately.

To give the reader an understanding in interpretation of the results that follow a glance at the theory is in order. Let X represent the matrix of discrepancies between the X-coordinates of the original grid and its reproduction via the tested film on a diapositive. The elements of the matrix X thus correspond positionally to the x-discrepancies at each grid intersection. Let Q be an orthogonal matrix whose rows are made up of values of orthogonal polynomials of ascending order. For uniformly spaced data, as is the case here, such values can be conveniently looked up in various tables (e.g., Fisher 1948, DeLury 1950).

Then

$$\boldsymbol{W} = \boldsymbol{Q}\,\boldsymbol{X}\,\boldsymbol{Q}^{T}$$

represents an orthogonal transformation of the observations which, given that the observations are independent and of equal variance, preserves their variance, i.e., the w_{ij}'s have the same distribution as the x_{ij}'s except that their mean is different. Let $\boldsymbol{Z}$ be a matrix which contains the squares of the elements of matrix $\boldsymbol{W}$, i.e., $\boldsymbol{Z} = (z_{ij}) = (w_{ij}^2)$. As an example, the $\boldsymbol{Z}_x$ and $\boldsymbol{Z}_y$ matrices represent typical results for the x- and y-discrepancies of one diapositive.

$$\boldsymbol{Z}_x = \begin{vmatrix} 68105613^* & 3760226^* & 13976^* & 1 & 4 & 0 & 0 \\ 7877^* & 75^* & 76^* & 8 & 0 & 1 & 3 \\ 1765^* & 2 & 5^* & 0 & 0 & 0 & 3 \\ 1003^* & 6 & 1 & 3 & 1 & 9 & 0 \\ 405^* & 20 & 1 & 10 & 3 & 1 & 0 \\ 112^* & 4 & 3 & 2 & 0 & 2 & 0 \\ 11 & 2 & 2 & 7 & 0 & 1 & 0 \\ 11 & 0 & 3 & 0 & 4 & 1 & 0 \end{vmatrix}$$

$$\boldsymbol{Z}_y = \begin{vmatrix} 1097316000^* & 11374^* & 13 & 0 & 0 & 4 & 0 \\ 3817270^* & 456^* & 0 & 1 & 2 & 2 & 5 \\ 0 & 883^* & 12 & 4 & 2 & 1 & 0 \\ 37 & 302^* & 6 & 9 & 0 & 3 & 1 \\ 21 & 122^* & 6 & 8 & 1 & 0 & 0 \\ 45 & 29 & 3 & 0 & 2 & 0 & 0 \\ 0 & 1 & 0 & 3 & 3 & 0 & 2 \\ 0 & 0 & 0 & 0 & 0 & 4 & 1 \end{vmatrix}.$$

Because of invariance of length under orthogonal transformation,

$$\sum_{ij} w_{ij}^2 = \sum_{ij} x_{ij}^2. \tag{7}$$

The total sum of squares of all the observations is thus divided into another set of squares, contained in matrix $\boldsymbol{Z}$, in such a way that each square now represents a dependence of the observations on a polynomial of certain degree in x and y. The strength of the dependence is reflected in the magnitude of the numbers. In our case, the numbers designated by asterisks stand above the rest and account practically for all the distortion of the film which thus takes the following polynomial forms in the x- and y- directions respectively:

$$d_x = a_{00} + a_{10}x + a_{01}y + a_{20}x^2 + a_{11}xy + a_{02}y^2 + a_{30}x^3 + a_{12}xy^2 + a_{40}x^4 + a_{50}x^5, \tag{8a}$$

$$d_y = b_{00} + b_{10}x + b_{01}y + b_{11}xy + b_{21}x^2y + b_{31}x^3y + b_{41}x^4y \tag{8b}$$

The remaining numbers in the $\boldsymbol{Z}$ matrices behave randomly as far as their magnitude is concerned and contribute only to the error sum of square. The sum of these numbers divided by their number thus provides an estimate of the variance of error. The respective standard errors in fitting the above polynomials to the transversal and longitudinal distortions are: $s_x = \pm 1.6$ μm and $s_y = \pm 2.2$ μm.

Equation 8a and 8b reveal a rather complex nature of the distortion. Subsequent scrutiny of the data uncovered a very unusual behaviour of the discrepancies along one marginal row of the grid which was completely inconsistent with the neighbouring row. No reason so far has been found for this unusual

pattern but the solution was repeated with the marginal grid lines left out, i.e., on the inner 18 by 18 cm format. The results improved drastically! In about 50 percent of the cases the decreased format showed no non-linear deformation and the remaining 50 percent displayed deformations expressible by much simpler forms than those given by Equations 8.

The preceding example points out the difficulty of compensating film distortion. Evidently, very little can be done with photographs with only four fiducial marks. Increasing the number of fiducial marks along the perimeter does not improve the situation very much, because such a location does not provide the necessary strength for reliable determination of coefficients of the required complex correction equations.

It has been our experience that the projective transformation Equations 9 give the most consistent results:

$$x = \frac{a_1x' + b_1y' + c_1}{dx' + ey' + 1}$$
$$y = \frac{a_2x' + b_2y' + c_2}{dx' + ey' + 1} \qquad (9)$$

In these equations x' and y' are the measured and x and y the calibrated values of fiducial mark coordinates. As the film distortion is very small, Equations 10a and 10b, which are an approximate form of Equations 9, may be used instead:

$$\delta x = a_0 + a_1x' + a_2y' + a_3x'y' + b_3x'^2 \quad (10a)$$
$$\delta y = b_0 + b_1x' + b_2y' + b_3x'y' + a_3y'^2. \quad (10b)$$

Here $\delta x = x' - x$ and $\delta y = y' - y$. These equations represent an exact one-to-one mapping of four fiducial marks and thus require, for their most efficiency, very precise determination of the coordinates of these points. It is a good practise to measure the calibration plate together with the diapositives on the same comparator and in the same position to eliminate comparator errors.

After compensation for film distortion by the proposed equations employing four simulated corner fiducial marks, errors larger than 10 microns were quite common which indicates an obvious inadequacy of the method. High local correlation of the residual displacements was evident.

Comparator Errors

Systematic errors can be imparted to image coordinates in the last instance by the comparator. Quite naturally, comparator errors depend on the type and construction of the instrument under consideration. Our experience has been only with a Wild STK-1 comparator and therefore this discussion is limited to the instruments of that type, namely those which utilize measuring screws.

The subject of screw-type comparator colibration is well documented in literature (e.g. Hallert 1963, Rosenfield 1963, Gugel 1965, Young 1968) and does not require additional attention except that the systematic errors normally discussed fail to take into account often severe errors arising during the operation of the instrument. As far as the errors associated with the lead screws and the guiding rails are concerned the instrument may be in a perfect adjustment as long as it is at rest. However, when in operation, unpleasant biases can arise. One of these is caused by the inevitable fluctuations of the internal temperature of the lead screws caused by friction. It would seem reasonable to demand that the manufacturers of such instruments provide some means to indicate the temperature changes of the spindles to the operator so that he may control his speed of turning the wheels. Changes in measured length of 26 cm of 3 to 4 microns originating from this cause were observed by Young (1968). Another bias observed on our instrument is the deflection of the y-carriage caused by translation of the px-carriage which it supports. This is especially apparent when changing from the *base in* to the *base out* positions.

Statistical Model for Coordinates

From the previous discussion it is obvious that our means of dealing with the systematic errors of image coordinates are, to say the least, inadequate. The coordinates, even after correction, must therefore still be regarded as afflicted by systematic errors and we can accordingly write for a general point:

$$x_i = \mu_{x_i} + \beta_{x_i} + \epsilon_{x_i}$$
$$y_i = \mu_{y_i} + \beta_{y_i} + \epsilon_{y_i}. \qquad (11)$$

where $(x, y)_i$ represent the improved coordinates of the point, $(\mu_x, \mu_y)_i$ their mean values, $(\beta_x, \beta_y)_i$ their unaccounted-for systematic error components and $(\epsilon_x, \epsilon_y)_i$ their error components.

The systematic components can be expressed as

$$\beta_{x_i} = f(x_i, y_i)$$
$$\beta_{y_i} = g(x_i, y_i) \qquad (12)$$

where f and g denote functions, unknown to us, which express the variation of these components within the picture format.

The random error components which include the sum of *all* elementary random errors are much smaller in magnitude. Their standard deviation, determined experimentally by Vlcek (1968), is estimated to lie between ± 1.5 and ± 2 microns for well defined images measured on precise comparators. It is quite safe to assume that these errors are distributed normally and independently with zero means. Their variances may not be homogeneous within the picture format but this situation can always be dealt with by a suitable weighting scheme.

The real problem therefore exists only with the systematic β-components. To regard these as statistical variables, we have to give them a stochastic character and define their probability distribution. We shall show that such a distribution can be created by *random* sampling of points within the region of the overlap. To this end let us consider, e.g., the component $\beta_x = f(x, y)$. Geometrically, we can think of this equation as a surface in 3-space. Let us cut this surface by a plane $\beta_x = \beta_o$. Then the probability that a randomly chosen point lies on the part of the surface below the secant plane $\beta_x = \beta_o$ is given by

$$P(\beta_x < \beta_0) = \frac{A_1}{A} = F(\beta_x) \qquad (13)$$

where A_1 is the area of the surface below the secant plane and A the total area within the bounds of the overlap. $F(\beta_x)$ has then the character of a distribution function, because for a low enough choice of β_o, e.g., $\beta_o = -50$ μm, whose size we do not admit on practical grounds, $F(\beta_x) = 0$ and for high enough value of β_o, e.g., $\beta_o = 50$ μm, $F(\beta_x) = 1$. Although the analytical form of $\beta_x = f(x, y)$ remains unknown, the distribution function $F(\beta_x)$ will be similar to the curve given in Figure 4 which represents the distribution function for a normally distributed variable.

Further, because the resulting systematic error is the sum of all elementary systematic errors, we can expect such a distribution to be reasonably symmetrical and with the mean value near zero.

We can now add the β- and ϵ-components and consider the distribution of their sum. It was found by this author and others by analyzing large samples of residual y-parallaxes after analytical model orientations that their distribution is indeed approximately normal with a near zero mean.

Summary and Conclusions

Significant systematic errors of image coordinates are a reality with which we must live now and likely continue to live for some time in the future, especially when we deal with photographs taken by the majority of contemporary cameras that employ film and are not equipped with a reseau. The presence of systematic errors leads to correlations, at least locally, among the coordinates, and introduces biases into orientation parameters with adverse consequences in strip and block solutions. The method proposed above which is based on the idea of random sampling of points will not eliminate the systematic errors but it should perform a very important function in that it will introduce randomness into orientation parameter errors and thus lead to a more favorable propagation within a strip or block assembly.

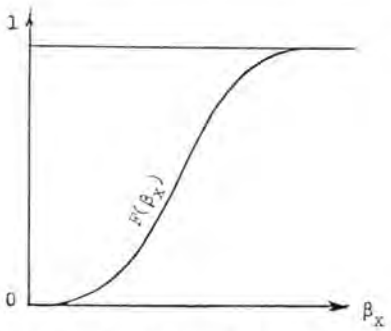

FIG. 4. The distribution function $F(\beta_x)$ will be similar to this curve which represents the distribution function for a normally distributed variable.

The main reason for randomization given by statisticians is that it establishes the validity of statistical tests by eliminating bias and thus makes it appropriate to analyze the data as though the errors were independent. In biological work neglect of proper randomization can especially lead to disastrous results. Our situation is not so bad but it would be interesting to learn how much improvement can be gained through this procedure in the analytical solution where the method is readily applicable. Of course, the choice of points cannot be completely left to chance, because the position of certain points, such as the pass points, is geographically limited to some degree within the overlap, but a certain amount of additional, randomly chosen orientation points could easily be introduced and this may well prove to be the area where the analytical solution will offer its greatest advantage to the photogrammetrist.

Acknowledgment

Some of the research mentioned was made possible through support by the National

Research Council and the Department of Energy, Mines and Resources in Ottawa.

References

Clark, J. M. T. "The Measurement of Film Flatness in Air Survey Cameras," Royal Aircraft Establishment, TR-64058, 1964.

Conrady, A. E. "Decentered Lens-Systems," *Monthly Notices of the Royal Astronomical Society* 79, 1919.

De Lury, D. B. "Values of Integrals of the Orthogonal Polynomials up to n=26," University of Toronto Press, 1950.

Epstein, I. L. "The Aberrations of Slightly Decentered Optical Systems," *Optical Soc. of America Jr.* 39, 10, 1949.

Fisher, R. A-F. Yates. "Statistical Tables for Biological, Agricultural and Medical Research," Oliver and Boyd, Edinburgh, 1948.

Gugel, R. "Comparator Calibration," PHOTO ENGINEERING, 31, 5, 1965.

Hallert, B. "Determination of the Precision and Accuracy of a Stereocomparator," *Schweizerische Zeitschrift für Vermessung, Kulturtechnik and Photogrammetrie*," 9, 1963.

Karren, J. R. "Camera Calibration by the Multicollimator Method," PHOTO ENGINEERING, 34, 7, 1968.

Maréchal, A. "Élude des aberrations d' excentrement," *Revue d'optique*, 29, 1, 1950.

Owen, C. "Optical Refractive Index of Air: Dependence of Pressure, Temperature and Composition," *App. Optics* 6, 1, 1967.

Rosenfield, G. H. "Calibration of a Precision Coordinate Comparator, PHOTO ENGINEERING, 29, 1, 1963.

Stephen, W. G. "Decentered Optical Systems," *App. Science Research* B 1, 1949.

Turner, J. B. "Image Coordinate Refinement in Analytical Photogrammetry," MASc Thesis, University of Toronto, 1967.

Vinklers, J. "An Experimental Study of the Dimensional Stability of An Aerial Film," MASc Thesis, University of Toronto, 1968.

Vlcek, J. "Analysis of Precision of Aerial Photographs and the Analytical Solution," Doctoral dissertation, University of Bratislava, 1968, (in Czech.).

Vlcek, J. "A Study of Analytical Models," PHOTO ENGINEERING, 33, 11, 1967.

Young, M. E. H. "Wild STK-1 Stereocomparator Calibration and Coordinate Refinement," MASc Thesis, Univ. of Toronto, 1968.

Book Review

A Descriptive Catalog of Selected Aerial Photographs of Geologic Features in Areas Outside the United States, assembled by Charles R. Warren, Dwight L. Schmidt, Charles S. Denny, and William J. Dale. Geological Survey Professional Paper 591. Superintendent of Documents. U.S. Government Printing Office, Washington, D. C., 20402. Printed in 1969.

The U. S. Geological Survey has selected and assembled sets of photographs of 67 of some of the more notable or representative geologic features that are to be found outside the United States. The catalog describes the features and lists the special sets of overlapping stereoscopic aerial photographs that are available for purchase. The sets of aerial photographs have been selected to illustrate a variety of geologic features in Antarctica, South and Central America, the Southwest Pacific, Iran, Japan, the Arabian Peninsula, Pakistan, and mainland China.

Teachers and students of the earth sciences will find the catalog a valuable aid in obtaining stereoscopic photographs of outstanding landforms and ice features. It tells how stereoscopic sets of 9-×9-inch vertical photographs and single high oblique photographs may be ordered, describes each feature and provides a sample 3-×3-inch photo of each of the 67 features.

A detailed description of the sets of photographs, including technical data of the photography is listed, country by country or region, including Antarctica. For many of the sets additional references are given to a topographic map and to a geologic map that covers the area. A small-scale pocket map gives the location of the aerial photographs in each country. Most of the Antarctic photographs are single high oblique photographs taken by the U. S. Antarctic Research Program sponsored by the National Science Foundation. Order forms and price information for the aerial photographs and maps are included.

Among the examples shown are ice and snow features in the Antarctic; an open pit copper mine in Chile; a glacier-clad equatorial volcano in Ecuador; khanat tunnels or water-collecting galleries of Iran; volcanos in Japan; and an astrobleme or meteor crater in Saudi Arabia.

The catalog is a companion publication to a descriptive catalogue of selected aerial photographs of geologic features in the United States: U. S. Geological Survey Professional Paper 590, published in 1968.

—*David Landen*